Power evolution along phase-sensitive parametric amplifiers: an experimental survey

Fatemeh Alishahi,[1,3,*] Armand Vedadi,[1] Mohammad Amin Shoaie,[1] Marcelo A. Soto,[2] Andrey Denisov,[2] Khashayar Mehrany,[3] Luc Thévenaz,[2] and Camille-Sophie Brès[1]

[1]*Photonic Systems Laboratory, Ecole Polytechnique Fédérale de Lausanne (EPFL), CH-1015 Lausanne, Switzerland*

[2]*Group for Fiber Optics, Ecole Polytechnique Fédérale de Lausanne (EPFL), CH-1015 Lausanne, Switzerland*

[3]*Electronics and Electrical Department, Sharif University of Technology, Azadi Ave., Tehran, Iran*

**Corresponding author: alishahi.fateme@gmail.com*

Received August 14, 2014; accepted September 16, 2014;
posted September 26, 2014 (Doc. ID 220988); published October 16, 2014

We propose and experimentally demonstrate a method based on Brillouin optical time-domain analysis to measure the longitudinal signal power distribution along phase-sensitive fiber-optical parametric amplifiers (PS-FOPAs). Experimental results show that the amplification of a PS-FOPA could go through different longitudinal profiles and yet finish with the same overall gain. This behavior is in sheer contrast with theoretical expectations, according to which longitudinal gain distribution should follow certain profiles determined by the initial relative phase difference but can never end up in the same overall gain. The gap between theory and experiment only becomes evident when the pump wavelength is within the fluctuation range of the zero dispersion wavelength (ZDW) of the PS-FOPA.

OCIS codes: (060.4370) Nonlinear optics, fibers; (290.5900) Scattering, stimulated Brillouin.
http://dx.doi.org/10.1364/OL.39.006114

A focus has been increasingly placed on fiber parametric devices by the research community [1,2]. In particular, phase-sensitive fiber-optical parametric amplifiers (PS-FOPAs) have received special attention for their distinguished noise figure which allows for a significant increase in channel capacity [1]. Since parametric amplification takes place while the signal propagates along the fiber, PS-FOPAs should be evidently considered as distributed elements. Still, in almost all previous experimental studies, the spectral characteristics of PS-FOPAs and their gain are measured solely at the output end of the fiber [2], neglecting the distributed nature of the amplifier in favor of a description of a lumped amplification process. In a lumped model, a PS-FOPA of length L is seen as an amplifier of gain G, whereas it is in fact made of an infinite number of cascaded amplifiers, each one corresponding to a PS-FOPA of an infinitesimal length dL. Although the overall gain of the amplifier is of foremost importance, the gain evolution along the fiber also matters to determine the amplifier performance. Actually, reordering the stages in cascaded amplifiers can severely affect the performance of the overall amplification process, in particular its noise characteristics, even though the total gain is the same [3].

It is therefore important to conceive a method to find the gain evolution along parametric amplifiers. The easiest way would be analyzing the basic scalar equations that describe the parametric amplification in terms of powers of pump, signal, and idler, as well as the relative phase difference between these waves [4]. However, the validity of these equations depends on assumptions that do not necessarily hold under experimental conditions. The limitations of the existing theory accentuate the necessity to conceive an experimental setup extracting the power distribution along fiber-optic parametric amplifiers. Depending on the phase difference between pump, signal, and idler at input of a PS-FOPA, different possible combinations of amplification (energy transfer from pump to signal/idler) and/or de-amplification (energy transfer from signal/idler to the pump) processes can occur along the fiber. These profiles may not be discernible from each other in conventional measurements, but they result in inherently different PS-FOPAs with properties depending on the amplification/de-amplification sequence experienced by the signal. The existence of different potential gain profiles to reach a certain gain in PS-FOPAs corroborates the fact that finding the overall gain is not enough for a complete characterization of PS-FOPAs, and measuring the gain evolution along the fiber is of crucial relevance.

To the best of our knowledge, Brillouin optical time domain analysis (BOTDA) [5] is the only nondestructive method that efficiently enables distributed measurements of power exchange for phase-insensitive fiber-optical parametric amplifiers (PI-FOPAs) [6]. In a nutshell, a pulsed parametric signal acts as a pump for Brillouin interaction with a counter-propagating continuous-wave (CW) probe [6]. However, the conventional BOTDA scheme of [6] faces two fundamental issues to measure the gain profile along PS-FOPAs. The first one is the power depletion that the parametric signal experiences as a result of the Brillouin interaction with the probe. The second is the nonlinear phase shift inflicted upon the signal when it is detuned from the center of Brillouin gain spectrum. Considering that the fiber can have unknown fluctuations of the Brillouin frequency, the phase of the signal can be significantly and unpredictably varied along the fiber. Indeed, the Brillouin-induced phase shift at the beginning of the fiber can severely impact on the measurement accuracy in PS-FOPAs due to the presence of idler at fiber input. For example, under good observation conditions and with typical power levels, even a deviation of only a few MHz in the Brillouin frequency shift over the first few meters of fiber span can cause up to 20% error in the measured gain distribution, as a result of the induced phase shift.

The scheme proposed in this Letter actually solves the two aforementioned points. The energy exchange in the proposed implementation is explained by the spectral

energy transfer diagram in Fig. 1. A high-power pump, a pulsed signal and its conjugated idler co-propagate in the fiber and interact through a phase-sensitive parametric process. Simultaneously, the pulsed signal interacts through Brillouin scattering with two counter-propagating probe sidebands. The success of the proposed scheme relies on two sideband probes of equal power that are positioned symmetrically with respect to the spectral position of the signal, with a pump-probe frequency offset matching the average Brillouin frequency shift Ω_B in the PS-FOPA. This way, the power that is transferred from the upper sideband probe to the signal compensates the signal power depletion induced by the power transfer to the lower sideband probe. Furthermore, the phase shift induced in the signal by its Brillouin interaction with the upper probe sideband is compensated by the interaction with the lower sideband, resulting in a null induced phase shift. This technique is very robust and the compensation is valid in spite of signal detuning from peak Brillouin gain frequency. The longitudinal evolution of the signal power, and thus the parametric gain along the PS-FOPA, is retrieved by measuring the variations of one of the probe sideband power in the time domain.

In contrast to our previous work [7], here a proper adjustment of the polarization states is required in some specific points of the implemented experimental setup (shown in Fig. 2), so that a good agreement between measurements and the scalar PS-FOPA theory can be ensured. The setup is composed of the following four main blocks: Parametric Waves Generation Block (PWGB), Probes Generation Block (PGB), Distributed Measurement Block (DMB), and Filtering and Detection Block (FDB).

The PWGB generates the parametric pump, signal, and idler waves for the phase-sensitive parametric amplification in the fiber under test (HNLF2 in the DMB). The parametric pump is generated using a CW-tunable laser (TL_1) followed by a phase modulator (PM) driven by a 10-GHz pseudo-random bit sequence (PRBS) of $2^7 - 1$ bits to suppress pump-induced SBS, and then amplified by an erbium-doped fiber amplifier (EDFA). A tunable 2-nm bandpass filter (TBF) is used to filter out the amplified spontaneous emission noise introduced by the EDFA. The pulsed signal is obtained by tapping 10% of another CW tunable laser (TL_2) power and directing it to a gated semiconductor optical amplifier (SOA) to produce 100-ns-wide pulses. The pump and pulsed signal are combined via a wavelength-division multiplexer (WDM) and pass through a polarizer and then a 99/1 coupler. The generated optical signals are then injected into a copier stage, where phase-insensitive parametric amplification generates the idler in HNLF1.

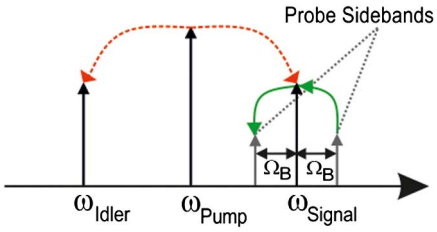

Fig. 1. Photon exchange diagram between pump, idler, signal, and probe sidebands. Parametric and Brillouin interaction are depicted by red (dash) and green (solid) arrows, respectively.

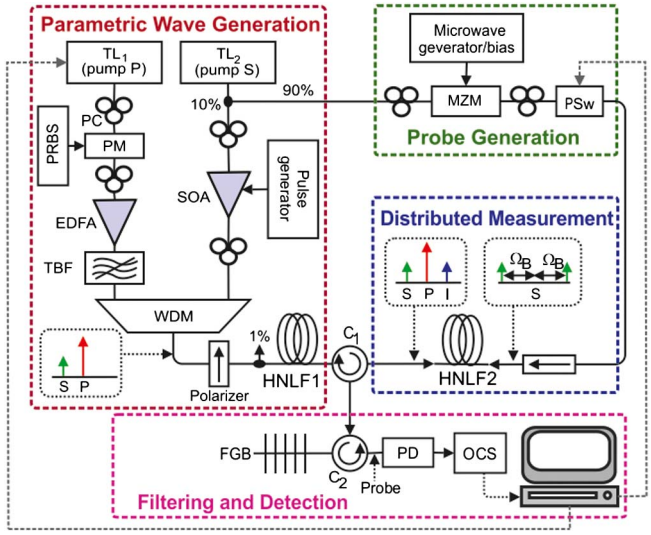

Fig. 2. Experimental setup. PC, polarization controller; PD, photodiode (all other acronyms are defined in the text). Dashed arrows indicate electronic command routes.

The PGB is based on intensity modulation by an RF tone to generate two symmetrical sideband probes: 90% of the power from TL_2 in PWGB is injected to a Mach–Zehnder modulator (MZM) driven at the Brillouin frequency and operating in high carrier suppression mode [8]. The polarization switch (PSw) is controlled by the computer to record traces with two orthogonal polarization states.

The DMB is the major block, wherein HNLF2 is used as a distributed PS-FOPA. The pump, the signal, and the idler from PWGB are launched from one end of the fiber, while the double-sideband probes from PGB are launched from the opposite end. After propagating along HNLF2, the probes pass through a circulator (C_1) to the FDB.

The FDB measures one of the probe components and processes the temporal traces to extract the PS-FOPA gain, ensuring that the extracted gain is compatible with scalar PS-FOPA theory, as described below. The gain extraction is performed in four steps. First, the TL_1 laser is turned on and the PSw is set to horizontal polarization. The parametric signal then interacts with the counter-propagating double-sideband probes within HNLF2. The sideband probe at frequency $\omega_{\text{signal}} - \Omega_B$ ($\omega_{\text{signal}} + \Omega_B$) experiences a local gain (loss) that is proportional to the local PS-FOPA signal peak power. Both probes are routed to the FDB through circulator (C_1). Using another circulator (C_2) together with a fiber Bragg grating (FBG), one of the probes is selected and directed to the monitoring oscilloscope (OSC). The temporal trace of the selected probe $P_H^{\text{ON}}(t)$ is recorded in the processing unit. In a second step, the entire process is repeated, this time by setting PSw to vertical polarization. The recorded trace is designated as $P_V^{\text{ON}}(t)$. The third and fourth steps are similar to the previous ones, but with the TL_1 turned off, so that there is no parametric amplification. The recorded traces are designated as $P_H^{\text{OFF}}(t)$ and $P_V^{\text{OFF}}(t)$ when the PSw is set to horizontal and vertical polarization states, respectively. Once these four steps are carried out, the quantities G_1 and G_2 are calculated as following:

$$G_1 = (P_H^{\mathrm{ON}}(t) + P_V^{\mathrm{ON}}(t))/(P_H^{\mathrm{OFF}}(t) + P_V^{\mathrm{OFF}}(t)), \quad (1a)$$

$$G_2 = 0.5 \times (P_H^{\mathrm{ON}}(t)/P_H^{\mathrm{OFF}}(t) + P_V^{\mathrm{ON}}(t)/P_V^{\mathrm{OFF}}(t)). \quad (1b)$$

Equation (1a) represents the scalar parametric gain cancelling out the polarization dependent Brillouin effects in the traces. Equation (1a) averages two parametric interactions at orthogonal polarizations and is expected to be equal to Eq. (1a). This expectation is supported by the fact that the parametric waves are co-polarized by passing through the polarizer in PWGB, and by the low birefringence in HNLF2, which facilitate co-polarized propagation of parametric waves, despite their wavelength separation. Nevertheless, the equality might not be held with a good accuracy because of partial nonlinear polarization rotation in nonscalar parametric interaction. To solve this issue, the entire procedure should be repeated by controlling the PCs in PWGB until $G_1 = G_2$ becomes a good approximation of the scalar parametric gain.

The experiment is conducted by using two typical HNLFs of length 500 m, designated HNLF1 and HNLF2. HNLF1 used in the copier stage is characterized by a typical end-to-end measurement method and has a ZDW at 1550 nm [9]. The ZDW of HNLF2 is reported as 1550 ± 5 nm by the manufacturer. Invoking the standard scalar theory for parametric amplification [4], the PS-FOPA gain along the fiber can be written as:

$$\begin{aligned} G_{\mathrm{PSA}}(z, \Delta\lambda) &= 1 + \gamma_2 P_2 \eta \sin(\theta(\Delta\lambda))/g_2 \sinh(2g_2 z) \\ &\quad + [\gamma_2^2 P_2^2 (1+\eta^2) + \gamma_2 P_2 \kappa_2 \eta \cos(\theta(\Delta\lambda))]/g_2^2 \sinh^2(g_2 z), \end{aligned} \quad (2a)$$

$$\theta(\Delta\lambda) = \frac{\pi}{2} + \tan^{-1}\left[\frac{\kappa_1}{2g_1}\tanh(g_1 L)\right] + \frac{2\pi c D_{\mathrm{SMF}} \Delta\lambda^2 L_{\mathrm{SMF}}}{\lambda_P \lambda_S}, \quad (2b)$$

where θ is the initial relative phase difference at HNLF2 input, η is the initial idler-to-signal-power ratio, λ_S and λ_P are the signal and the pump wavelengths, P_2 is the undepleted pump power, γ_2 is the nonlinear coefficient of HNLF2, L is the HNLF1 length, and L_{SMF} and D_{SMF} are the total length and dispersion of the pigtails between HNLF1 and HNLF2, respectively. Also, $\Delta\lambda$ is the difference between signal and pump wavelengths, and c is the vacuum light velocity. Note that for a high gain copier stage FOPA, it is possible to assume $\eta = 1$. Also, κ_i and g_i $(i = 1, 2)$ stand for the phase matching and linear parametric gain within HNLFi, respectively. Equation (2a) could be seen as either gain spectra or longitudinal gain distribution leading to either a lumped or distributed interpretation of the PS-FOPA, respectively. To examine both of these aspects, the pump wavelength is tuned to $\lambda_P = 1556.4$ nm, i.e., outside the ± 5 nm ZDW range of fluctuations in HNLF2, and the experiment is carried out at ten different signal wavelengths between 1547.8 and 1548.7 nm. Figure 3(a) shows the overall gain measured at the output of the PS-FOPA (red circles) and compares it against the theoretically obtained gains $G_{\mathrm{PSA}}(z = 500, \Delta\lambda; \lambda_S, \lambda_P = 1556.4\ \mathrm{nm})$ in Eq. (2a) (black solid line). The initial relative phase difference, calculated from Eq. (2b), is also depicted in this figure as a function of the signal wavelength. Figure 3(a) points out that the overall gain spectrum is symmetrically centered on a gain hole at the signal wavelength of 1548.3 nm. The PS-FOPA gain distributions corresponding to five selected wavelengths in Fig. 3(a) are measured by the proposed experimental setup and are plotted using solid lines in Fig. 3(b). The PS-FOPA gain distributions corresponding to other wavelengths have been omitted in Fig. 3(b) for clarity, since they overlap with the already shown gain distributions.

Figure 3(b) shows (in dashed lines) the theoretically obtained PS-FOPA gain distributions $G_{\mathrm{PSA}}(z, \Delta\lambda = \lambda_{\mathrm{P}} - \lambda_{\mathrm{Si}})$, in which λ_{Si} is the ith wavelength indicated in the figure. Results point out an excellent agreement between the theory and the experiment. It is important to notice that the theory predicts three distinct types of gain distributions and thereby discerns phase-sensitive from phase-insensitive amplifiers [10]. An analysis of the theoretical gain in Eq. (1a) reveals that there is always one local minimum whose position is at:

$$z_0 = \tanh^{-1}[\eta \sin(\theta)/(2(1+\eta^2) + \eta\gamma_2 P_2 \kappa_2 \cos(\theta))]/2g_2. \quad (3)$$

Evidently, z_0 could be at or before the beginning of the fiber ($z_0 \le 0$), outside the fiber span ($z_0 \ge L$), or somewhere in between. These different cases define three distinct types of gain distributions that can be respectively designated as pure amplification, pure de-amplification, and de-amplification followed by amplification. Contrarily, in a PI-FOPA where $\eta = 0$, the only possible pattern is pure amplification since $z_0 = 0$. In our experiment, pure amplification along the entire HNLF2 is observed at the signal wavelength of 1547.8 nm, where the initial relative phase difference is $\theta = 3\pi/5$. Pure de-amplification is observed at the signal wavelength of 1548.3 nm, where the initial relative phase difference is $\theta = -9\pi/10$. Actually, the direction of photon transfer

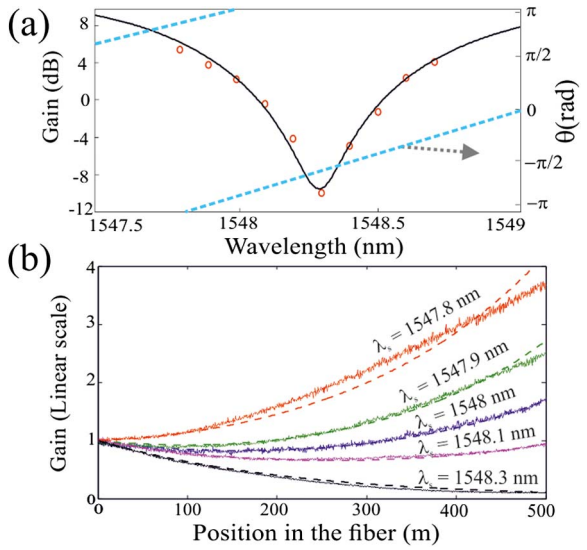

Fig. 3. (a) Left vertical axis: theoretical (solid curve) and experimental (circles) phase sensitive overall gain. Right vertical axis: calculated initial relative phase shift. (b) Experimental (solid curve) and theoretical (dashed curve) gain evolutions.

in parametric interaction is determined by the sign of the initial relative phase shift between pump(s), signal, and idler [4], such that a positive/negative sign of this phase shift results in pure amplification/de-amplification. The longitudinal PS-FOPA gain evolutions corresponding to the remaining signal wavelengths in Fig. 3(b) illustrate the third pattern, i.e., the de-amplification followed by amplification. This pattern shows that once the inversion of energy flow has occurred at z_0, it does not invert further until depletion begins. The study of three typical gain profiles reveals that while an initially negative phase difference becomes positive at certain fiber position z_0, a positive phase difference never becomes negative. That is why amplification is never expected to be followed by de-amplification if there is no external perturbation affecting the system.

Theory and experiment validate each other through the previously presented results. However, they do not agree when the pump wavelength lies within the range of ZDW fluctuations in HNLF2. This is here demonstrated by repeating the experiment, this time with the pump wavelength tuned to 1551.3 nm. Figure 4(a) shows the overall gain measured for different signal wavelengths at the output of the PS-FOPA (circles). As before, the overall gain spectrum is symmetric with respect to the gain hole. Still, a striking difference between this and the former experiment emerges when the longitudinal PS-FOPA gain distributions are examined. On one aspect, the experimentally extracted gain distributions at signal wavelengths 1527.2 and 1527.9 nm are astoundingly different from each other even though their overall gain values are nearly the same. For another aspect, the experimentally extracted gain distributions do not necessarily fit in the three theoretically predicted categories of gain distributions. These two differences are clearly seen from Fig. 4(b), where the PS-FOPA gain distributions, corresponding to three different signal wavelengths (1527.2, 1527.5, and 1527.9 nm), are plotted. Comparison of the gain distribution at signal wavelengths 1527.2 and 1527.9 nm supports the fact that the PS-FOPA can reach a specific overall gain following different profiles: amplification followed by de-amplification or vice versa. Given that the discrepancy between theory and experiment does not appear until the pump wavelength lies within the uncertainty range of ZDW, we believe the difference is reconcilable. If the generalized nonuniform PS-FOPA theory is considered [10], a PS-FOPA of length L can be taken as an infinite number of cascaded infinitesimal PS-FOPAs of length dL. Since each infinitesimal PS-FOPA in this approach has uniform characteristics and thus can follow any of the three theoretically predicted gain distributions, the observed profile within the total length L does not necessarily stick to one of the expected profiles and rather could be quite disordered. It is worth noting that these types of unexpected profiles are never observed in a PI-FOPA, where pure amplification is the only possible gain profile outside the ZDW fluctuation range.

In conclusion, a robust experimental method has been proposed to extract the longitudinal gain evolution along the PS-FOPA, which is designed to have negligible effect on the amplitude and phase response of the amplifier. The proposed approach is important from two aspects. First, it provides an experimental criterion for evaluation

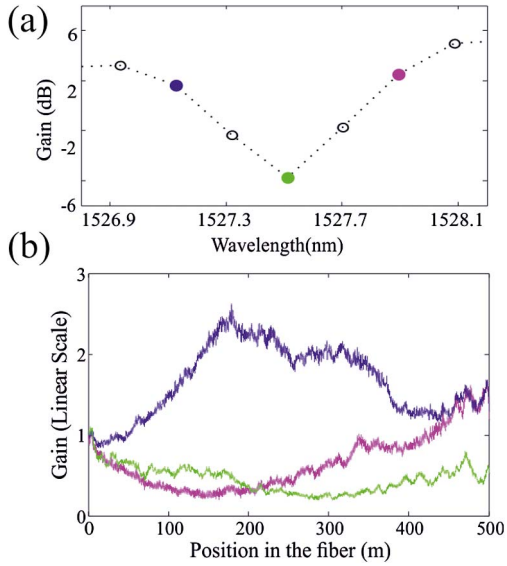

Fig. 4. (a) Experimental (circles) overall gain. (b) Experimental gain evolution at particular signal wavelengths: 1527.2 nm (blue), 1527.5 nm (green), and 1527.9 nm (pink).

of the accuracy of the basic scalar equations that describe the phase-sensitive parametric amplification in terms of optical powers and relative phase difference [4]. The experimental results are in a perfect agreement with the theory when the pump wavelength is far from the ZDW. Second, the experiment shows that when the amplifier is tuned within the fluctuation range of ZDW, the PS-FOPA supports different amplification profiles having the same overall gain. This finding has no parallel in PI-FOPA and can be of considerable interest if the performance of PS-FOPA is to be evaluated precisely.

Authors would like to acknowledge T. Sylvestre from Femto-ST Besançon for providing the tested fiber. This project was in part funded by Marie Curie CIG No. 303700.

References

1. Z. Tong, C. Lundström, P. A. Andrekson, C. J. McKinstrie, M. Karlsson, D. J. Blessing, E. Tipsuwannakul, B. J. Puttnam, H. Toda, and L. G. Nielsen, Nat. Photonics **5**, 430 (2011).
2. J. Kakande, C. Lundström, P. A. Andrekson, Z. Tong, M. Karlsson, P. Petropoulos, F. Parmigiani, and D. J. Richardson, Opt. Express **18**, 4130 (2010).
3. M. E. Marhic, Opt. Express **20**, 28752 (2012).
4. R. Tang, J. Lasri, P. S. Devgan, V. Grigoryan, P. Kumar, and M. Vasilyev, Opt. Express **13**, 10483 (2005).
5. T. Horiguchi and M. Tateda, J. Lightwave Technol. **7**, 1170 (1989).
6. A. Vedadi, D. Alasia, E. Lantz, H. Maillotte, L. Thévenaz, M. Herráez, and T. Sylvestre, IEEE Photon. Technol. Lett. **19**, 179 (2007).
7. F. Alishahi, A. Vedadi, M. A. Soto, A. Denisov, K. Mehrany, L. Thévenaz, and C. Brès, in *Proceedings of the Optical Fiber Communication Conference* (Optical Society of America, 2014), p. Th1H.4.
8. M. Niklès, L. Thévenaz, and P. A. Robert, Opt. Lett. **21**, 758 (1996).
9. B. Auguie, A. Mussot, A. Boucon, E. Lantz, and T. Sylvestre, IEEE Photon. Technol. Lett. **18**, 1825 (2006).
10. M. E. Marhic, *Fiber Optical Parametric Amplifiers, Oscillators and Related Devices* (Cambridge University, 2008).